Journal of the European Ceramic Society 35 (2015) 4513–4520

Contents lists available at www.sciencedirect.com

Journal of the European Ceramic Society

journal homepage: www.elsevier.com/locate/jeurceramsoc

Mechanical characterisation of a fibre reinforced oxide/oxide ceramic matrix composite

D.T. Di Salvo [a], E.E. Sackett [a], R.E. Johnston [a], D. Thompson [b], P. Andrews [c], M.R. Bache [a,*]

[a] Institute of Structural Materials, College of Engineering, Swansea University, Bay Campus, Swansea SA1 8EN, UK
[b] Cytec Industrial Materials (Derby) Limited, Heanor, Derbyshire DE75 7SP, UK
[c] Rolls-Royce plc, P.O. Box 31, Derby DE24 8BJ, UK

ARTICLE INFO

Article history:
Received 14 August 2015
Accepted 25 August 2015
Available online 2 September 2015

Keywords:
CMC
Oxide–oxide
Mechanical properties
Failure mechanisms
Component lifing

ABSTRACT

Monotonic tension, fatigue and creep experiments were conducted on an oxide/oxide ceramic matrix composite over the range of temperature 20–1200 °C. The role of continuous fibre reinforcement, differential thermal expansion, stress redistribution interactions between fibres and matrix and the influence of inherent processing defects are all considered when describing the deformation and ultimate mechanical failure of these systems.

1. Introduction

High performance engineering designs for land based power generation systems and aero-engine applications continue to drive research into ceramic composites, mainly due to their high temperature capability which ultimately offers increased operating temperatures [1]. In the aerospace sector their low density provides attractive specific properties with the potential for reductions in component weight. Recent interest in oxide/oxide ceramic matrix composite systems (CMCs) originates from superior oxidation behaviour when compared to non-oxide based variants (e.g. SiC_f/SiC or SiC_f/Al_2O_3), which is particularly apparent at temperatures above 800 °C [2,3]. Additional benefits in the combined costs of raw materials, processing technologies and component manufacture should also be considered [4]. The successful implementation of oxide/oxide CMCs for structural applications will require a compromise in mechanical performance compared to the competing non-oxide systems, where SiC_f/SiC is currently viewed as the industry leader. However, this should not avert interest in the oxide/oxide systems.

Our recent research has assessed an oxide/oxide CMC under three important loading configurations, namely monotonic tension, low cycle fatigue and creep over a range of temperatures. This form of assessment constitutes a vital pre-requisite to component design and potential service lifing. Constitutive stress–strain behaviour, fatigue and creep strength were defined together with a detailed understanding of the micro-mechanisms controlling deformation and fracture in this CMC. All of these properties were considered in relation to the structural condition of the as-processed materials.

2. Experimental procedures

Continuous fibre reinforced oxide/oxide CMC material stocks were manufactured by a proprietary process at Cytec Ltd. Flat panels of nominal dimensions 120 mm × 120 mm and 3.5 mm thickness were produced utilizing Nextel™ 720 alumina-based fibres embedded in an alumina matrix. The twelve plies of single weave mats contained fibres in 0/90° orientations. Specimens with a parallel gauge section were machined from the panels utilizing diamond tooling, with their longitudinal axis parallel to the nominal 0° fibre orientation. The same specimen design was employed for all tensile, fatigue and creep testing (Fig. 1).

For all forms of testing, specimens were carefully aligned to avoid bend and torsional stresses during insertion into the load train and subsequent loading. For all high temperature tests a short, two zone MTS radiant furnace was employed, with specimen temperature monitored using calibrated R type thermocouples, to ensure uniform heating over the measured gauge length. Tensile

* Corresponding author.
E-mail address: m.r.bache@swansea.ac.uk (M.R. Bache).

http://dx.doi.org/10.1016/j.jeurceramsoc.2015.08.032

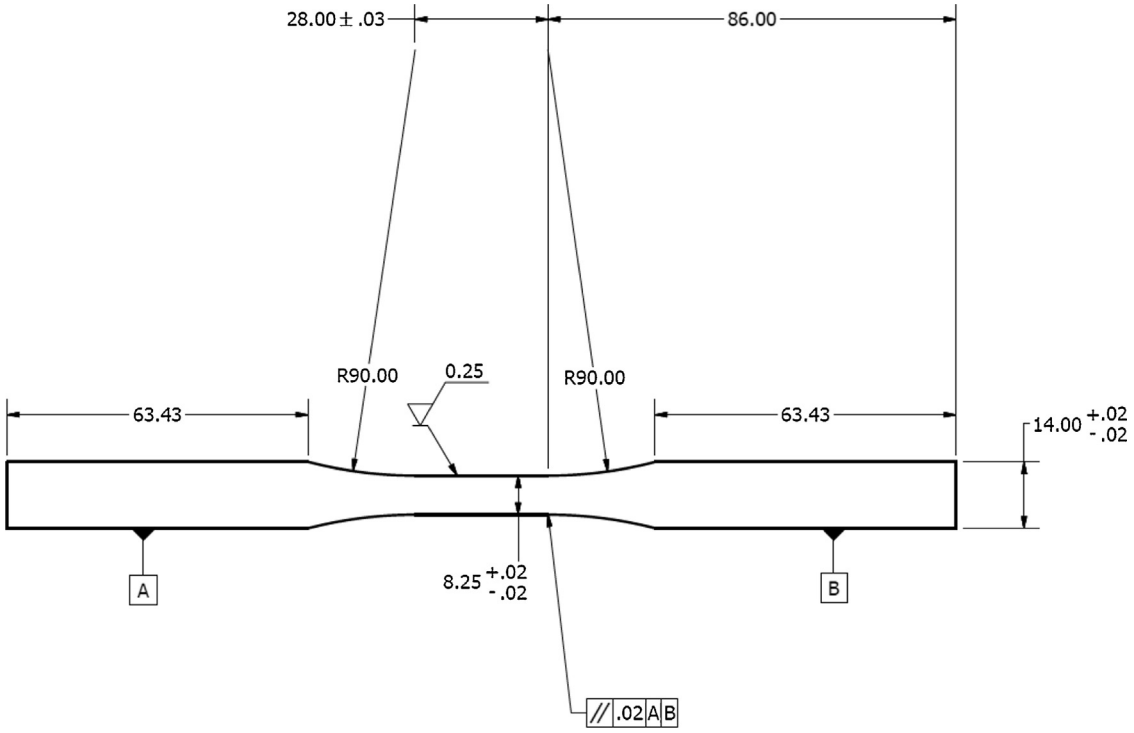

Fig. 1. Specimen design.

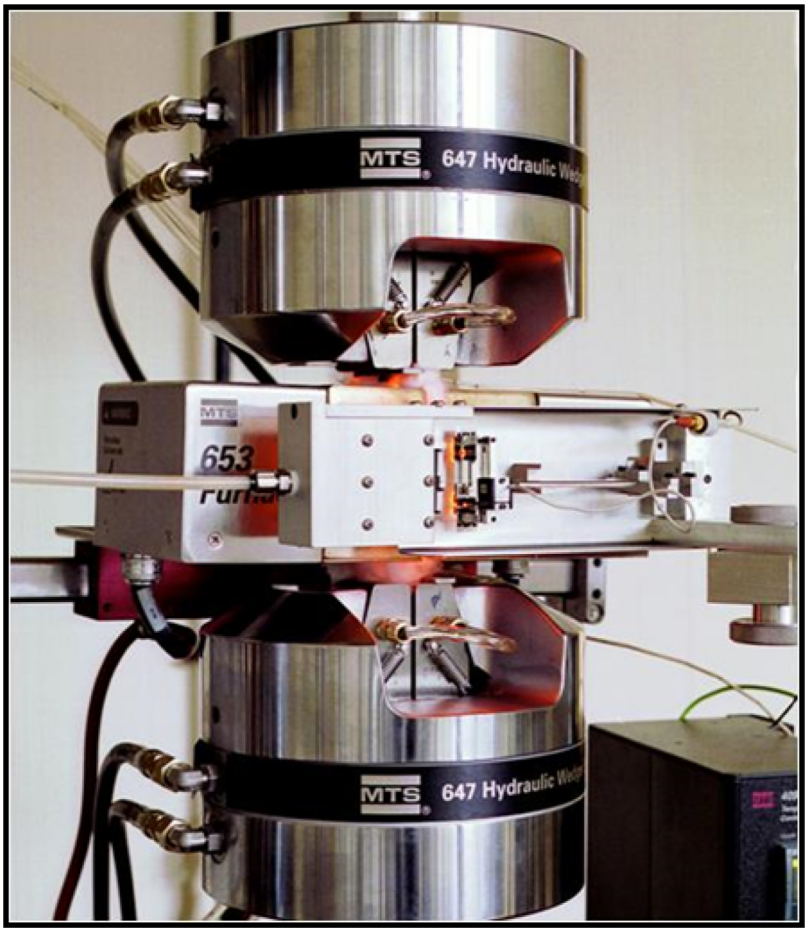

Fig. 2. Experimental facility for performing tensile and fatigue tests.

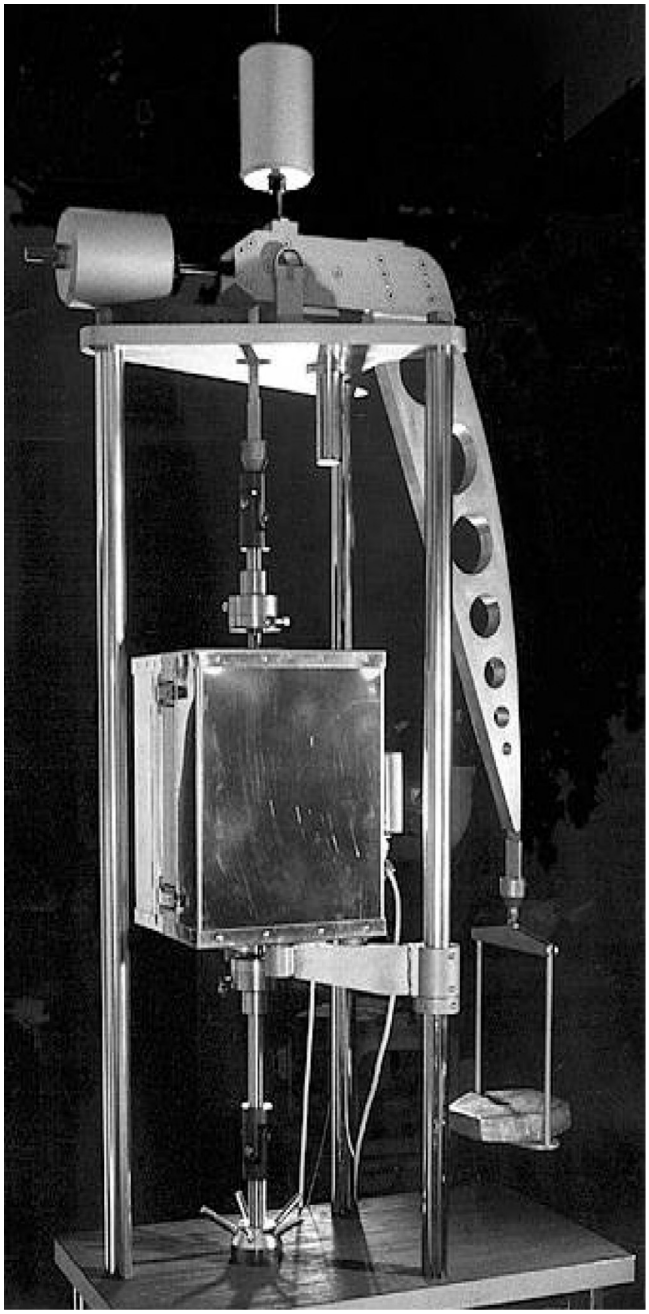

Fig. 3. Constant stress creep frame for CMC testing.

tests were carried out in accordance with ASTM C1275-10 & C1359-11 [5,6], under position control at 1 mm per minute. A commercial MTS high temperature strain gauge bridge extensometer, with an initial gauge length of 25 mm, was used to measure tensile strain directly from the gauge section. Fatigue tests were performed under load control and utilized a 15 cpm trapezoidal waveform (1 s linear rise and fall ramps with a 1 s hold at both peak and minimum load) with $R = 0.1$; according to ASTM C1360-10 [7]. The general experimental setup for tensile and fatigue tests, utilizing hydraulic wedge grips outside of the slim furnace, is shown in Fig. 2. Creep tests were performed to ASTM C1337-10 [8] using constant stress rigs (Fig. 3), but on this occasion employing mechanical wedge grips exposed to room temperature either side of a MTS split furnace.

Ruptured specimens were inspected using a range of optical and scanning election microscopes.

Table 1
Mechanical property data.

ID	Test temperature (°C)	UTS (MPa)	Strain to failure
RT#1	20	172	0.0030
RT#2	20	163	0.0028
RT#3	20	179	0.0030
RT#4	20	170	0.0031
RT#5	20	167	0.0028
HT#1	1150	207	0.0034
HT#2	1150	212	0.0036

3. Results

3.1. Monotonic tension

Monotonic tensile tests were performed at 20 °C and 1150 °C (five and two tests respectively) as an initial assessment of basic strength and mechanical repeatability. Specimens were deliberately selected to sample different CMC panels at random locations within each, i.e. some were taken near the panel edges and others in the mid sections. The constitutive response at either temperature is illustrated by two typical stress–strain curves in Fig. 4. Irrespective of test temperature, the early stages of the stress–strain curve were remarkably similar in all seven tests. A distinct, proportional elastic regime was absent during each test, rather, the slope of the stress-strain curve gradually decreased with increased loading. Table 1 collates pertinent mechanical data from the test matrix to illustrate the degree of reproducibility. The ultimate tensile strength at either temperature was consistent between specimens to within 10 MPa. Notably, an increased UTS was measured at 1150 °C with a slight improvement in strain to failure relative to the room temperature data. At either temperature, rupture occurred in an instantaneous fashion with restricted fibre pull out.

3.2. Low cycle fatigue

Low cycle fatigue data, generated at 20 °C and 1150 °C, are plotted as SN curves in Fig. 5. At both temperatures, the SN curve is relatively flat, with a small change in applied peak stress resulting in a wide range of cyclic life. At specific peak stress conditions, repeat testing helped identify a large degree of scatter in cyclic performance. The slope of the SN curve appears similar across the temperature range, highlighted by the trend lines superimposed by eye. Similar to the response noted under monotonic loading, an increase in fatigue strength was observed with increasing test temperature. In general, when inspecting the failed specimens, a greater degree of 0° fibre pull-out parallel to the loading axis was evident at elevated temperature while the fracture zone within the room temperature specimens was more restricted (Fig. 6). At either temperature, significant decohesion between transverse 90° fibre bundles and the matrix was often noted (Fig. 7a). Similar decohesion was also evident between longitudinal 0° fibres and the local matrix at high magnification (Fig. 7b). It was never possible to identify a specific, single site for crack initiation.

3.3. High temperature creep

Stress–rupture data representing constant-stress creep tests performed at temperatures ranging from 1100 to 1200 °C are presented in Fig. 8. The data demonstrate a classical inverse relationship between creep strength and temperature. Best fit trend lines have been superimposed by eye, to highlight the change in the slope to the apparent stress–rupture curve at 1200 °C, consistent with the limiting temperature capability of such oxide/oxide systems [2]. A typical creep failure is illustrated in Fig. 9, demonstrating relatively minor fibre pull out parallel to the loading axis. At

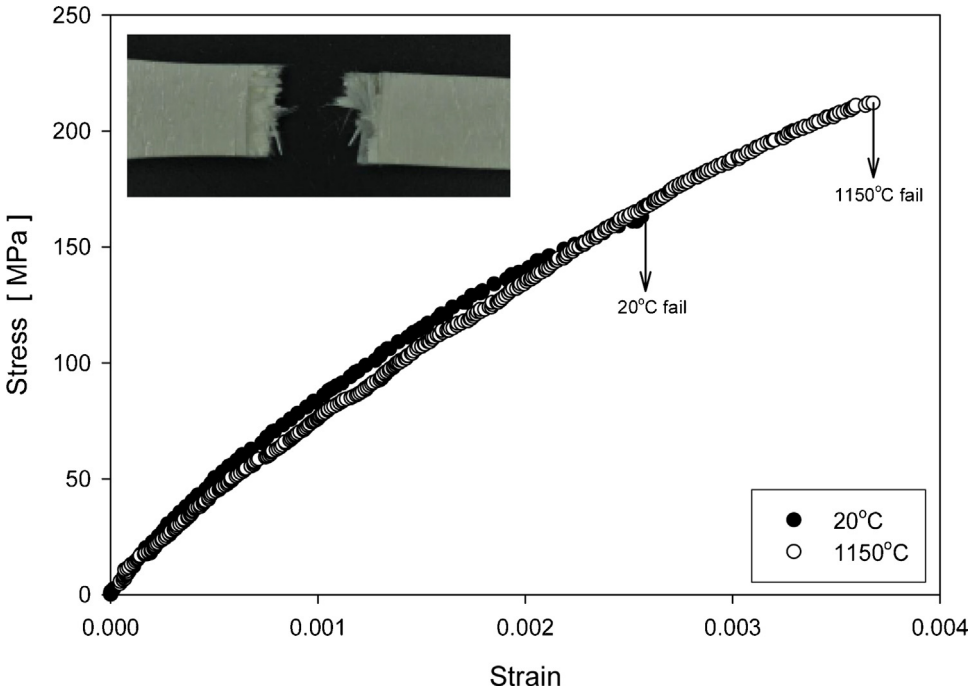

Fig. 4. Monotonic tensile data, 20 °C and 1150 °C (with typical fracture illustrated at 1150 °C).

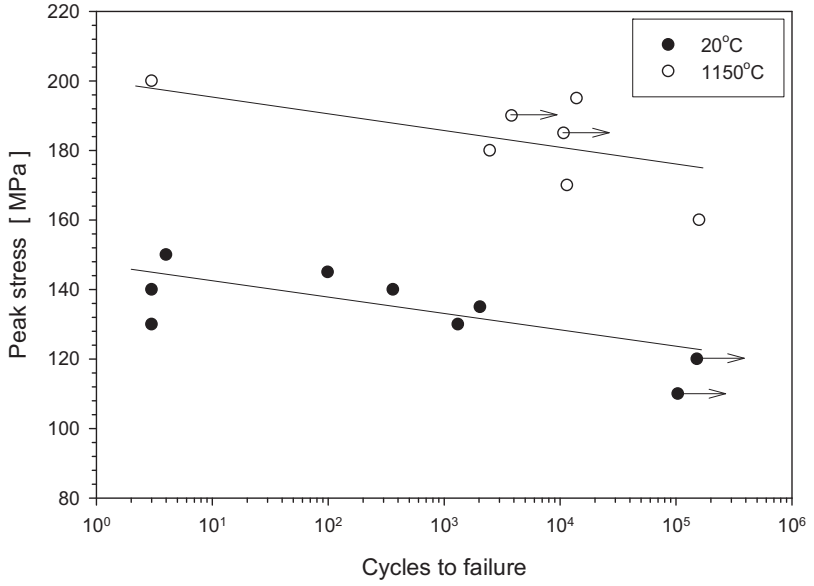

Fig. 5. LCF response at 20 °C and 1150 °C, $R = 0.1$, 15 cpm.

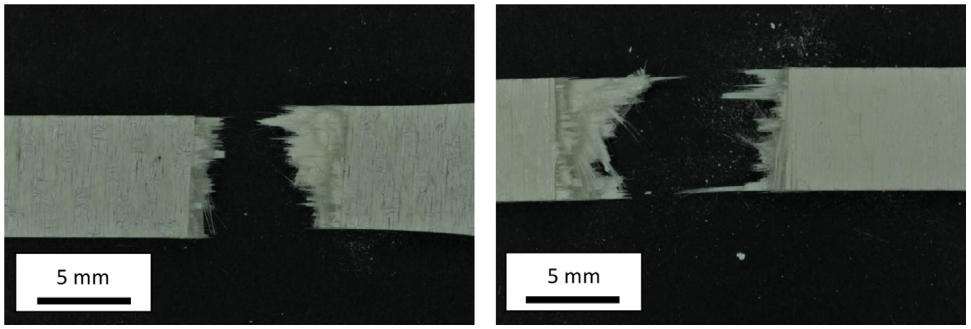

Fig. 6. Typical LCF fractures at room temperature (left) and 1150 °C (right).

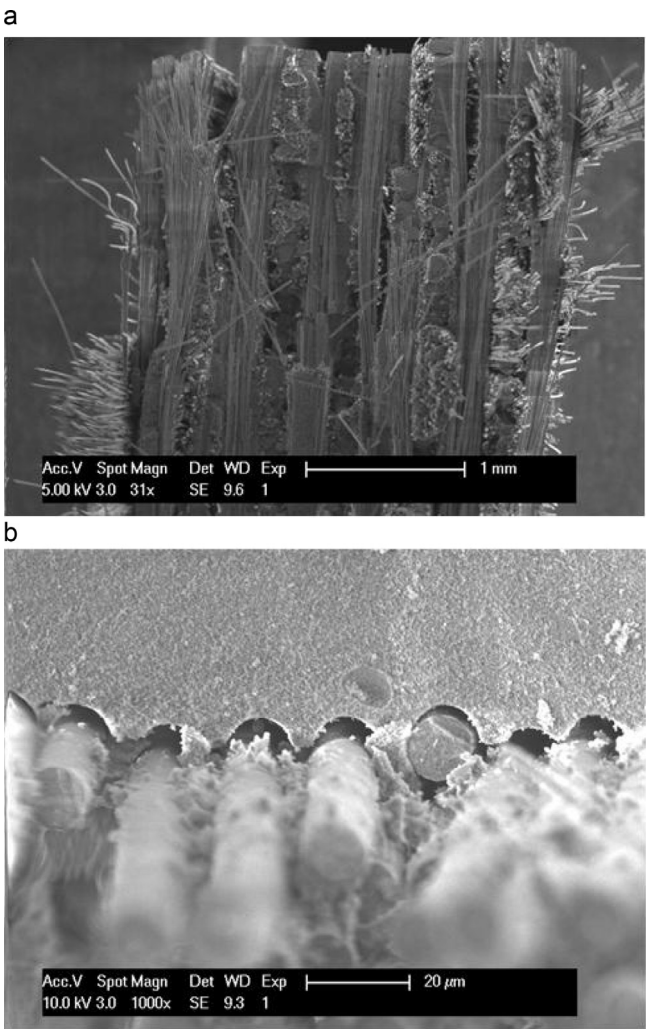

Fig. 7. (a (top)) Macroscopic plan view of a LCF fracture surface generated at 1150 °C, illustrating transverse 90° fibre bundle decohesion from the matrix. (b (bottom)) Local decohesion between longitudinal 0° fibres and matrix generated at 1150 °C (i.e. tensile stress out of page).

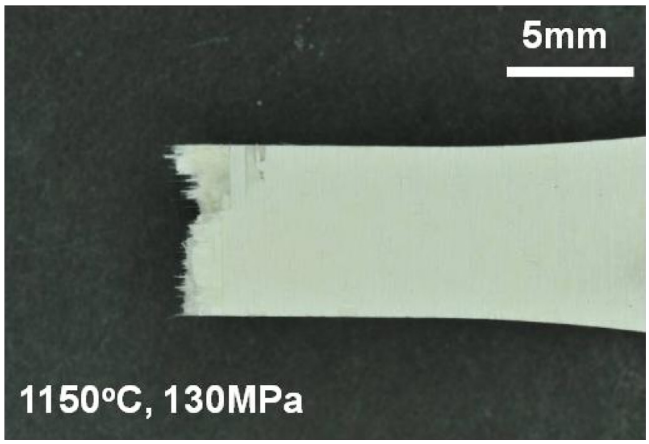

Fig. 9. Typical creep failure, generated at 130 MPa, 1150 °C.

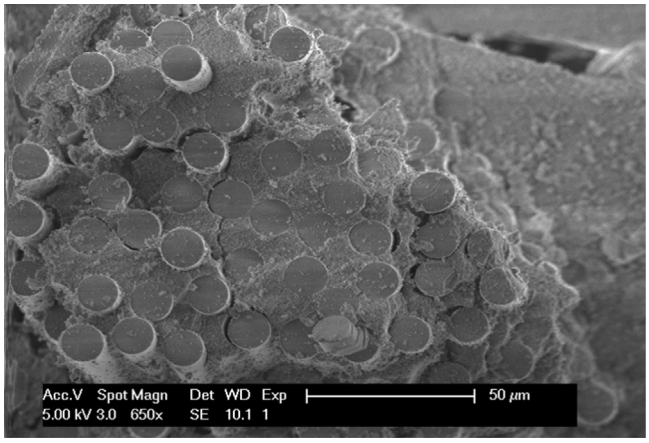

Fig. 10. Brittle creep fracture extending across a longitudinal 0° fibre bundle (common across the range of temperatures assessed).

higher magnification (Fig. 10), a relatively flat, brittle appearance is illustrated by fractures traversing through localized bundles of longitudinal fibres. Individual fibres demonstrate virtually featureless fracture surfaces, orientated perpendicular to the applied tensile

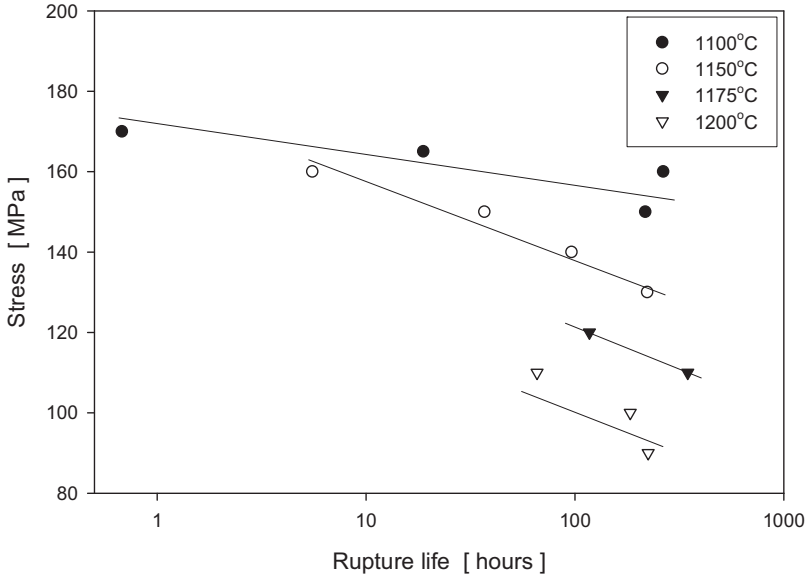

Fig. 8. Stress–rupture creep data for the range of temperature 1100–1200 °C.

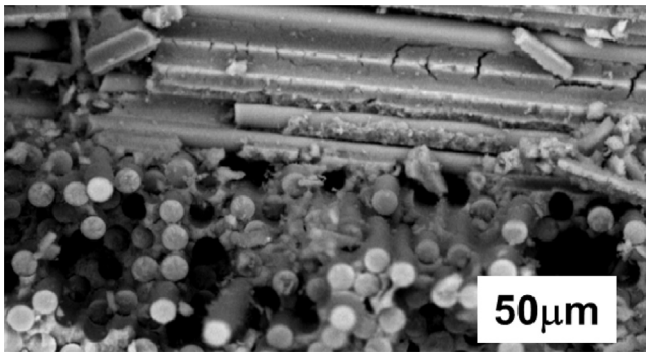

Fig. 11. Micro-cracking exposed by displaced transverse fibres.

stress, with no evidence of the local direction of crack growth. Also note from this image the fine debris covering the fracture surface. This is an artifact of the relatively friable matrix phase. No obvious deformation was detected away from the plane of fracture and the adjacent damage zone.

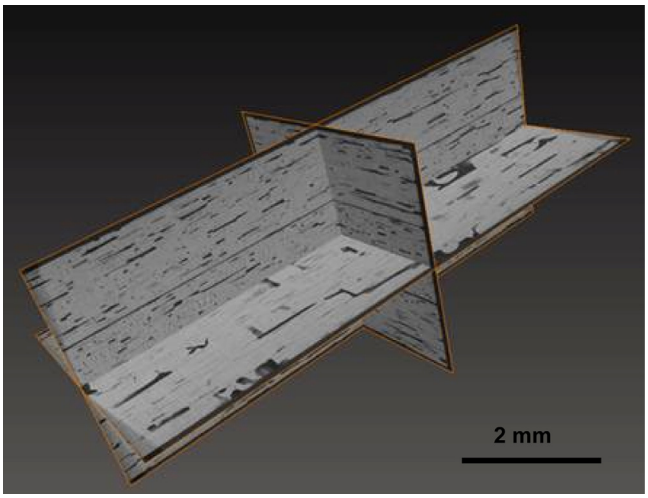

Fig. 12. Computed tomography images on three intersecting, orthogonal planes through a randomly selected material volume.

4. Discussion

The mechanism of failure in these oxide–oxide materials is naturally complex. Firstly, it should be emphasised that the current materials represented the earliest attempts to produce this particular CMC system using standard industrial scale equipment and practice. Prior to this study, the system had been formulated and assessed in the laboratory, employing techniques similar to some previously reported [9]. Therefore, the parameters employed here for fibre weaving, fibre mat lay-up, slurry infiltration, firing and consolidation all remain open to optimisation. Therefore, crucial from the mechanical performance viewpoint, the interfacial properties between the matrix and fibre constituents have yet to receive detailed consideration. Evidence has been noted from the various fracture surfaces of regions where the bonding between fibres and matrix was particularly weak, demonstrated by the clean channels exposed when transverse fibres pull out of the matrix (Figs. 7 and 11). The length of longitudinal fibre pull-out was variable from test to test, with a maximum pull-out length of approximately 5 mm witnessed under tensile loading. The length of this pull out was noticeably greater under cyclic fatigue loading compared to static creep. This may indicate that damage accumulation is more diffuse under fatigue with early cracking concentrated within the matrix phase leading to widespread instances of fibre bridging.

The non destructive characterisation of the composite has shown a relatively high volume of inherent porosity exists within the material, present as a combination of meso-scopic cavities between the individual fibres and fibre tows and fine scaled microscopic pores within the matrix. These stress concentrating features should act as potent crack initiators under reversible fatigue loading cycles. Differences in elastic stiffness and subsequent decohesion between the two phases can induce fibre buckling during the unloading portion of the fatigue cycle. These forms of failure mechanism have been widely reported for a range of CMC systems [10,11]. The restricted length of fibre pull out in the creep specimens suggests a more concentrated region of damage evolves under static stress. This evolution of strain “hot spots” in CMCs under creep conditions has been previously recorded at room temperature using advanced strain mapping techniques [12] and it is assumed that a similar mechanism would occur at high temperature subject to potential modifications through enhanced oxidation and stress relaxation. Clearly, the opportunity for reversed damage is absent during static loading.

The presence of post processing residual stress between the fibres and matrix, originating from a disparity in thermal expansion and local constraints during sintering, and the alleviation of this stress through exposure to high temperature was previously proposed as an explanation why the monotonic tension and fatigue strengths of this CMC were greater at elevated temperature compared to room temperature [13]. Circumstantial evidence for the post processing stress is noted in Fig. 11, where the removal of transverse fibres from the matrix during ultimate failure often revealed small scale cracks within the matrix but orientated at angles near parallel to the axis of loading. The direct relationship measured on this current oxide/oxide CMC between ultimate tensile strength and temperature was also noted during previous research reported for a competing oxide/oxide system [14]. From the present findings it is now evident that a similar relationship extends to low cycle fatigue strength. The limiting, highest temperature for this relationship has yet to be defined, however, considering previous studies this is likely to occur somewhere above 1200 °C [2]. The restriction in fibre pull out, illustrated by fatigue failures in Fig. 6 but also seen under monotonic tension, providing a relatively flat, brittle fracture at room temperature, supports this argument. Relatively easy decohesion between fibres and the matrix, either as transverse bundles or individual longitudinal fibres (Fig. 7a and b), has been demonstrated across the temperature range assessed. It should be emphasized that the current CMC materials remain in the early stages of development and improvements to the matrix-fibre interface could now be considered to improve “toughness” by encouraging an optimised degree of fibre bridging and ultimate fibre pull out.

Over the period of assessment, the as processed panels contained approximately 27% porosity by volume, measured by computed tomography and image analysis. Fig. 12 illustrates the underlying composite structure on three intersecting orthogonal planes within a nominal volume of material. Fig. 13 then emphasizes the presence of interlaminar discontinuities in a two dimensional CT section taken through a stack of three test coupons prior to mechanical assessment. Notably, these interlaminar features should have a relatively minor effect on mechanical properties measured across the plane of the processed panel, however, it is suspected that their influence on interlaminar shear and even through thickness axial strength would be significant. The scale of the pores, resulting from incomplete matrix consolidation and gas entrapment between individual and fibre tows, ranged from sub-micron up to a few millimetres for the worst cases of

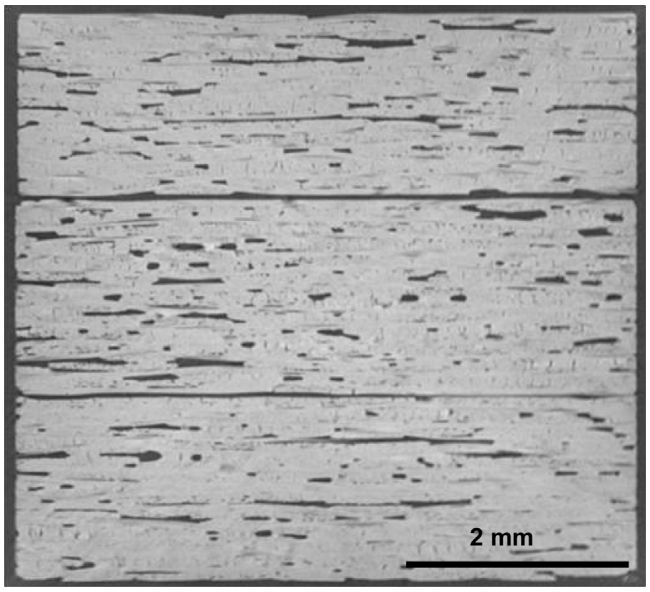

Fig. 13. Two dimensional CT sections through a stack of three test coupons.

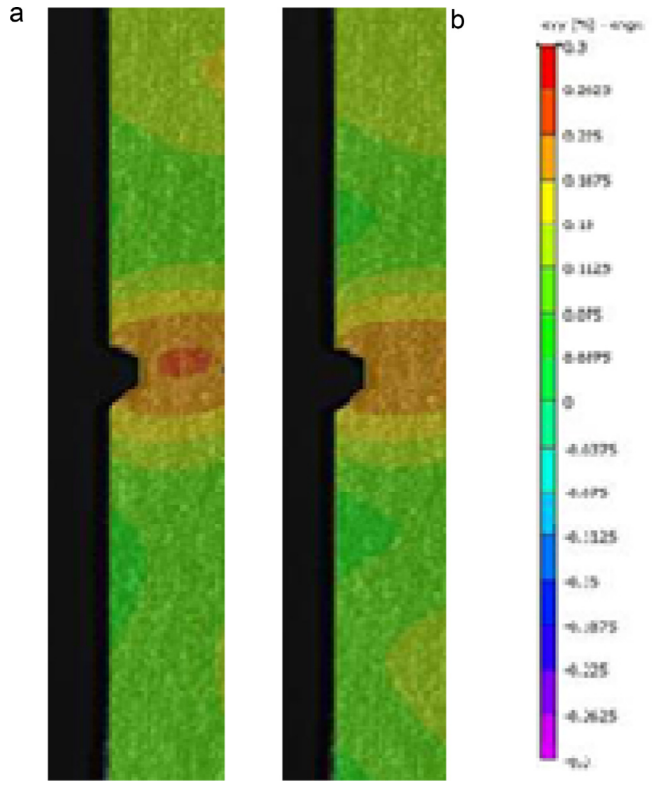

Fig. 14. Stress relaxation at a notch feature under monotonic tensile loading (image A followed by B).

interconnected porosity [15]. It is assumed that failures will initiate from a significant pore (or multiple sites) within the material, although depending on precise shape and location this may not always implicate the largest scale feature. At room temperature, crack growth then appears to remain on a relatively flat plane. The exact flaw to initiate failure under any form of mechanical test is usually impossible to define on the fracture surface, given the extremely complex structure of this class of CMC and high volume fracture of inherent porosity and processing defects. The more substantial fibre pull out seen at elevated temperature is consistent with an increase in interfacial decohesion and more efficient redistribution of stress between matrix and fibres under these conditions.

Under static creep loading, a classical inverse relationship was defined between creep strength and temperature. Simple inspection by eye was usually sufficient to distinguish creep fractures from those generated under fatigue, with much reduced fibre pull out evident under static loading. This is in contrast to evidence from alternative silicon carbide matrix based systems [16]. Contemporary studies using digital image correlation to monitor damage accumulation in the same oxide/oxide CMC under static loading at room temperature have demonstrated that deformation remains widely distributed throughout the composite until immediately prior to fracture, where damage is restricted to a relatively localized region either side of the eventual fracture plane [17]. Cyclic fatigue appears to distribute damage across a wider volume leading to enhanced fibre-matrix delamination and individual fibre pull-out.

In terms of engineering design, both the fatigue SN curve and creep stress–rupture curves are relatively flat, with only minor changes in applied stress producing significantly different lives to failure. This agrees with previous reports [18,19]. The stochastic nature of the material inherently induces a large amount of scatter amongst both the fatigue and creep life data. Simply from the viewpoint of generating the required mechanical database to support component design and lifing activities, this can provide challenges for laboratory testing. The non-proportional constitutive response measured under monotonic loading, together with the damage mechanisms highlighted during the present research, illustrate a degree of "pseudo-plasticity" in this CMC. However, the associated energy dissipation remains limited. From an engineering design perspective, a simple "safe stress" approach is recommended, defining the endurance condition (whether under cyclic or static load) and applying an appropriate safety factor.

To further support engineering design, the effects of macroscopic stress raising features such as holes and notches, often incorporated to CMC architectures to enable fixturing between components, must also be assessed for local damage accumulation and fracture behaviour. A lack of significant "notch sensitivity" on static strength and the associated fractography appears to demonstrate that any localised stress raising effect of these geometric features does not affect the mechanism of failure [20]. The longitudinal 0° fibres should be responsible for distributing the applied loads through the section of the coupon and early measurements using digital image correlation appear to demonstrate the concentration of stress at the notch root redistributes readily (see Fig. 14). This example illustrates how the region of peak induced stress immediately inboard of a notch actually reduces under incremental monotonic loading at room temperature. Ongoing fatigue studies using double edge notch specimens have shown that cyclic loading also fails to induce a significant stress concentration or K_t effect. This is an important finding when considering component designs.

5. Conclusions

The following high level conclusions can be drawn from the present study:

- An oxide–oxide CMC material of current interest offers reasonable mechanical properties for selected engineering applications, despite a reduction in temperature capability when compared to silicon carbide based systems.
- A direct relationship between strength and temperature was defined up to 1150 °C under monotonic and cyclic loading, apparently controlled by the post processing residual stress state between matrix and fibres.

- A relatively high volume fraction of post processing porosity exists in these slurry infiltrated CMC materials, making definition of the exact site of mechanical failure impossible.
- A "safe stress" approach to component design and service lifing is proposed.

Acknowledgements

The current research was funded by the UK Engineering and Physical Science Research Council, research grant TS/G000484/1, with an additional EngD stipend for DTDS. The provision of materials by Cytec Ltd. and their technical support in collaboration with Rolls-Royce plc are gratefully acknowledged.

References

[1] J.A. DiCarlo, M. van Roode, Ceramic composite development for gas turbine engine hot section components, in: ASME Turbo Expo 2006: Power for Land, Sea and Air, Barcelona, Spain, 2006.
[2] D.B. Marshall, J.B. Davis, Curr. Opin. Solid State Mater. Sci. 5 (2001) 283–289.
[3] D.M. Wilson, L.R. Visser, High performance oxide fibers for metal and ceramic composites, in: Processing of Fibers and Composites Conference, Barga, Italy, 2000.
[4] J.E. Lane, J.A. Morrison, B. Marini, C.X. Campbell, Hybrid oxide-based CMCs for combustion turbines: how hybrid oxide CMC mitigates the design hurdles typically seen for oxide CMC, in: ASME Turbo Expo 2007: Power for Land, Sea and Air, Montreal, Canada, 2007.
[5] ASTM C1275-10, Standard Test Method for Monotonic Tensile Behavior of Continuous Fiber-Reinforced Advanced Ceramics with Solid Rectangular Cross-Section Test Specimens at Ambient Temperature, ASTM International.
[6] ASTM C1359-11, Standard Test Method for Monotonic Tensile Strength Testing of Continuous Fiber-Reinforced Advanced Ceramics With Solid Rectangular Cross-Section Test Specimens at Elevated Temperatures, ASTM International.
[7] ASTM C1360-10, Standard Practice for Constant-Amplitude, Axial, Tension–Tension Cyclic Fatigue of Continuous Fiber-Reinforced Advanced Ceramics at Ambient Temperatures, ASTM International.
[8] ASTM C1337-10, Standard Test Method for Creep and Creep Rupture of Continuous Fiber-Reinforced Advanced Ceramics Under Tensile Loading at Elevated Temperatures, ASTM International.
[9] C. Kaya, F. Kaya, E.G. Butler, A.R. Boccaccini, K.K. Chawla, Development and characterisation of high-density oxide fibre-reinforced oxide ceramic matrix composites with improved mechanical properties, J. Eur. Ceram. Soc. 29 (June (9)) (2009) 1631–1639.
[10] G. Fantozzi, P. Reynaud, Mechanical hysteresis in ceramic matrix composites, Mater. Sci. Eng.: A 521–522 (2009) 18–23.
[11] B. Wilshire, M.R. Bache, Creep of monolithic and fibre-reinforced silicon carbide, J. Eur. Ceram. Soc. 28 (7) (2008) 1535–1542.
[12] E. Sackett, M.R. Bache, Damage accumulation under static and fatigue loading in a SiC_f/Al_2O_3CMC, in: Negro (Ed.), Proceedings of CIEC 9, Bardonechia, Italy, 2004, ISBN 888202010X, 9788882020101.
[13] M.R. Bache, R.E. Johnston, P. Andrews, I.M. Edmonds, A mechanical assessment of oxide–oxide CMC materials, in: Proceedings of CIEC 12, Mons, Belgium, 2010.
[14] S.G. Steel, Monotonic and fatigue loading behaviour of an oxide/oxide ceramic matrix composite, Masters thesis, Air Force Institute of Technology, Wright Patterson Air Force Base, Dayton, Ohio, 2000.
[15] R.E. Johnston, M.R. Bache, M. Amos, D. Liaptsis, R. Lancaster, R. Lewis, P. Andrews, I.M. Edmonds, Investigation of non-destructive evaluation methods applied to oxide/oxide fibre reinforced ceramic matrix composite, in: ICACC, 22–27 January 2012, Daytona Beach, USA, 2012.
[16] M.R. Bache, Fracture and durability assessment of materials, components and structures, in: Proceedings of Fatigue, EIS, Sheffield, UK, 2003.
[17] D.T. di Salvo, M.R. Bache, N. Banerjee, Damage accumulation in CMC systems under static loading, in: Anglada, Garcia, Jimenez-Pique, Mestra (Eds.), Proceedings of CIEC 13, Barcelona, Spain, 2012, ISBN 978-84-615-9681-2.
[18] C.A.Eber, Effect of temperature and steam environment on fatigue behaviour of an oxide-oxide continuous fiber ceramic composite, Masters thesis, Air Force Institute of Technology, Wright Patterson Air Force Base, Dayton, Ohio, 2005.
[19] P.A. Koutsoukos, Effects of environment on creep behaviour of two oxide-oxide ceramic matrix composites at 1200 C, Masters thesis, Air Force Institute of Technology, Wright Patterson Air Force Base, Dayton, Ohio, 2006.
[20] M.R. Bache, S. Hillier, D.T. di Salvo, P. Andrews, D. Thompson, Oxide/oxide ceramic matrix composites—mechanical assessment of stress raising features and simple sub-element geometries, in: Gadow, Kern (Eds.), Proceedings of CIEC 14, Stuttgart, Germany, 2014, ISBN-13: 978-3844029758.